

Provided by the author(s) and University of Galway in accordance with publisher policies. Please cite the published version when available.

Title	Ignition studies of n-heptane/iso-octane/toluene blends
Author(s)	Javed, Tamour; Lee, Changyoul; AlAbbad, Mohammed; Djebbi, Khalil; Beshir, Mohamed; Badra, Jihad; Curran, Henry J.; Farooq, Aamir
Publication Date	2016-07-09
Publication Information	Javed, Tamour, Lee, Changyoul, AlAbbad, Mohammed, Djebbi, Khalil, Beshir, Mohamed, Badra, Jihad, Curran, Henry J., Farooq, Aamir. (2016). Ignition studies of n-heptane/iso-octane/toluene blends. Combustion and Flame, 171, 223-233. doi: http://dx.doi.org/10.1016/j.combustflame.2016.06.008
Publisher	Elsevier ScienceDirect
Link to publisher's version	http://dx.doi.org/10.1016/j.combustflame.2016.06.008
Item record	http://hdl.handle.net/10379/6096
DOI	http://dx.doi.org/10.1016/j.combustflame.2016.06.008

Downloaded 2024-05-28T11:04:37Z

Some rights reserved. For more information, please see the item record link above.



Ignition studies of n-heptane/iso-octane/toluene blends

Tamour Javed¹, Changyoul Lee², Mohammed AlAbbad¹, Khalil Djebbi¹, Mohamed Beshir¹, Jihad Badra³,
Henry Curran², Aamir Farooq^{1*}

¹ Clean Combustion Research Center, King Abdullah University of Science and Technology, Thuwal, Kingdom of Saudi Arabia

² Combustion Chemistry Centre, National University of Ireland Galway, Galway, Ireland

³ Fuel Technology Division, R&DC, Saudi Aramco, Dhahran, Kingdom of Saudi Arabia

*Corresponding author email: Aamir.farooq@kaust.edu.sa

Abstract

Ignition delay times of four ternary blends of n-heptane/iso-octane/toluene, referred to as Toluene Primary Reference Fuels (TPRFs), have been measured in a high-pressure shock tube and in a rapid compression machine. The TPRFs were formulated to match the research octane number (RON) and motor octane number (MON) of two high-octane gasolines and two prospective low-octane naphtha fuels. The experiments were carried out over a wide range of temperatures (650 – 1250 K), at pressures of 10, 20 and 40 bar, and at equivalence ratios of 0.5 and 1.0. It was observed that the ignition delay times of these TPRFs exhibit negligible octane dependence at high temperatures ($T > 1000$ K), weak octane dependence at low temperatures ($T < 700$ K), and strong octane dependence in the negative temperature coefficient (NTC) regime. A detailed chemical kinetic model was used to simulate and interpret the measured data. It was shown that the kinetic model requires general improvements to better predict low-temperature conditions and particularly requires improvements for high sensitivity (high toluene concentration) TPRF blends. These datasets will serve as important benchmark for future gasoline surrogate mechanism development and validation.

Keywords: TPRF surrogates; RON; MON; Ignition delay times; Shock tubes; RCMs

1. Introduction

Commercial transportation grade gasoline is widely used for light duty vehicles, and is a complex mixture of hundreds of hydrocarbons, primarily spanning C_4 – C_{10} , including linear and branched paraffins, naphthenes, olefins and aromatics [1]. The composition of gasoline may vary considerably depending on its origin and refining/upgrading process [2]. State-of-the-art advanced combustion engine (ACE) technologies, such as homogeneous charge compression ignition (HCCI), reactivity controlled compression ignition (RCCI), gasoline compression ignition (GCI), premixed charged compression ignition (PCCI) and their variants, are expected to be more efficient [3, 4], and will have a reduced environmental footprint associated with hydrocarbon combustion [5]. Fuel reactivity and ignition characteristics are the fundamental parameters controlling ignition in these ACE technologies [6-8]. Therefore, the development and validation of chemical kinetic mechanisms for gasoline-like fuels is very important. Due to the complex composition of gasoline, or any real fuel for that matter, it is an arduous task to assemble a chemical kinetic mechanism for all of the constituents. This difficulty is overcome by formulating a simple surrogate fuel which emulates the target properties of the real fuel. Generally, these target properties include the desired combustion properties (ignition delay, flame speeds, etc.) and/or physical properties (molecular weight, H/C ratio, viscosity, density, distillation curve, etc.). However, it should be noted that a given surrogate may not be able to emulate all of the targets and, therefore, care must be taken in selecting a particular surrogate. Good accounts on surrogate fuel formulation strategies can be found in [8-14].

Primary reference fuel (PRF) surrogates are among the simplest surrogates employed to emulate gasoline ignition. A PRF is a bi-component mixture of *n*-heptane (octane number defined to be 0) and iso-octane (octane number defined to be 100), with PRF xx meaning xx% iso-octane and 1 – xx% *n*-heptane by volume. Gasoline fuels are knock rated, having both a Research Octane Number (RON) and a Motor Octane Number (MON), based on comparisons with PRF blends in a cooperative fuels research (CFR) engine. Due to the traditional use of *n*-heptane and iso-octane as gasoline surrogate components, several experimental [15-17] and modeling efforts [18-21] are available in the literature describing the ignition of *n*-heptane and iso-octane. A few chemical kinetic modeling and experimental studies have also focused on describing the ignition of PRF blends [16, 22-27].

It has been shown that a PRF surrogate captures the ignition of a high-paraffinic content gasoline reasonably well at temperatures above 850 K [28]. Sarathy et al. [28] showed that for two highly paraffinic gasoline fuels, FACE (Fuels for Advanced Combustion Engines; Conoco Philips) gasoline A and C, a PRF surrogate was more reactive at low temperatures (< 850 K) compared to the gasoline fuels. Commercial gasoline fuels generally have high aromatic content ($\sim 20 - 30$ %) and some other non-paraffinic ($\sim 5 - 10$ %) components [1]. Consequently, such fuels tend to have a high sensitivity ($S = \text{RON} - \text{MON}$) which can be thought of as a measure of the non-paraffinic content of the fuel. A PRF surrogate by definition has zero sensitivity and will not be able to emulate the ignition behavior of a real gasoline fuel. Kalghatgi and coworkers [13, 14] demonstrated that PRF surrogates cannot be used to rate a gasoline based on the primitive RON and MON testing methods. This discrepancy is due to the fact that real gasoline, due to its high sensitivity ($S \sim 10$), matches different PRF blends at different engine operating conditions. They proposed the use of toluene/*n*-heptane [14] and toluene/*n*-heptane/iso-octane [13] blends as more suitable gasoline surrogates. Kalghatgi et al. [13] developed correlations to calculate the composition of a toluene/*n*-heptane/iso-octane surrogate to match the RON and sensitivity of a target gasoline for a wide range of octane numbers. By matching both RON and sensitivity, the surrogate is expected to capture the real fuel reactivity over a wide range of conditions.

There have been a few fundamental ignition studies of surrogates comprising three or more components. Gauthier et al. [29] studied the auto-ignition characteristics of *n*-heptane/air, RD387 gasoline/air, and ternary surrogate/air (63% iso-octane / 20% toluene / 17% *n*-heptane by volume) mixtures in a shock tube facility. They showed that the auto-ignition behavior of the RD387 gasoline was well-reproduced by the ternary surrogate. Vanhove et al. [23] studied an iso-octane/1-hexene/toluene ternary blend in a rapid compression machine, interestingly preferring 1-hexene over *n*-heptane to produce low-temperature reactivity. Kukkadapu et al. [30] measured ignition delay times of RD387 in a rapid compression machine and the results agreed well with the work of Gauthier et al. [29]. In further studies, Kukkadapu et al. [31, 32] reported better agreement of a four component (iso-octane/*n*-heptane/toluene/2-pentene) surrogate with ignition delay times of RD387 at lower temperatures compared to the ternary surrogate proposed by Gauthier et al. [29]. Sarathy et al. [28] used five- (*n*-butane/iso-pentane/2-methylhexane/*n*-heptane/iso-octane) and six- (*n*-butane/iso-pentane/2-methylhexane/*n*-heptane/toluene/iso-

octane) component surrogates to simulate low-temperature ignition of FACE gasolines A and C, respectively.

Previous work has thus shown that ternary blends of toluene/*n*-heptane/iso-octane (henceforth referred to as TPRF) can serve not only as adequate gasoline surrogate candidates on their own but may also be major constituents of the more complex multi-component surrogates. This is because TPRF surrogates can emulate the aromatic, *n*-paraffinic and iso-paraffinic content present in a real gasoline, where these three classes represent > 90% of the chemical content of commercially available distillate gasoline fuels. However, wide-ranging fundamental studies of TPRF ignition and chemical kinetic development are not available in the literature. The objective of the current work is to provide a large dataset of experimental ignition delay times of TPRF blends for use in the refinement and development of surrogate kinetic models. Here, ignition delay times of four TPRF mixtures (RON = 70, 80, 91 and 97.5; S = 4, 5.7, 7.6 and 10.9) have been measured in a shock tube (ST) and in a rapid compression machine (RCM). These measurements were performed at pressures of 10 (RCM), 20 and 40 bar (RCM and ST) in the temperature range 650 – 1250 K and at equivalence ratios of 0.5 and 1.0. The TPRF mixtures were formulated to match the RON and sensitivity of two certified gasoline and two prospective naphtha-like fuels. These data are the first of their kind and will form highly valuable dataset for future gasoline surrogate mechanism development and validation.

2. Methods

2.1. TPRF Surrogate Formulation

Several methodologies have been proposed in the literature to formulate TPRF surrogates for gasoline fuels [13, 33, 34]. Morgan et al. [33] developed a second-order volume-based model to derive TPRF surrogate composition corresponding to the RON and MON of the target fuel. Kalghatgi et al. [13], on the other hand, proposed a second-order method on molar basis. Both works relied on engine octane data to optimize the correlations. Pera et al. [34] used octane ratings and the carbon, hydrogen and oxygen content of the target gasoline (ULG 95) to optimize the TPRF surrogate. However, they used linear by volume blending method which can potentially introduce errors in determining surrogates composition [33]. The TPRF surrogates studied in this work were formulated based on the correlations developed by Kalghatgi et al. [13]. These correlations calculate the TPRF surrogate composition required to emulate the RON

and sensitivity the target fuel. The surrogates tested in this work were formulated over a wide range of octane numbers (RON: 70 – 97.5) with varying degrees of sensitivity (S: 4 – 11). The RON and MON values of the TPRF surrogates were experimentally measured at the Saudi Aramco Research and Development Center in their cooperative fuel research (CFR) engine following the ASTM D6733 (RON) and D6730 (MON) standards. These surrogates are listed in Table 1. It can be seen that the measured and estimated (from [13]) RON and MON values are in very good agreement with each other which further fortifies the use of the correlations developed by Kalghatgi et al. [13]. For brevity, the surrogate blends henceforth will be referred as TPRF xx where xx represents the RON of the surrogate blend.

Table 1: TPRF surrogates investigated in this work. See Table S1 (Supplementary Material) for compositions in mole fractions.

Surrogate	iso-octane ¹	<i>n</i> -heptane ¹	Toluene ¹	RON estimated ²	RON measured ³	MON estimated ²	MON measured ³	Sensitivity ⁴
TPRF 70	42.48	36.23	21.29	70	70	66	66	4
TPRF 80	39.85	28.58	31.57	80	80.4	74.3	75.3	5.7
TPRF 91	36.58	19.31	44.1	91	92	83.4	84.3	7.6
TPRF 97.5	11.52	18.04	70.44	97.5	98	86.6	87.1	10.9

¹ % volume

² RON and MON estimated using correlations developed by Kalghatgi et al. [13]

³ RON and MON measured in a CFR engine using ASTM standards

⁴ Sensitivity S = RON – MON (estimate)

2.2. Experimental Details

The experiments reported in this study were performed in the high-pressure shock tube (HPST) facility at King Abdullah University of Science and Technology (KAUST) and in a rapid compression machine (RCM) at the National University of Ireland, Galway (NUIG). Both of these facilities have previously been described in the literature [35] and only a brief overview is given here.

The HPST at KAUST is constructed from stainless steel with an inner diameter of 10 cm. The driven section is 6.6 m long and the driver section has a modular design to vary its length from 2.2 m to a maximum of 6.6 m. The mid-section of the tube houses two pre-scored aluminum diaphragms in a double-diaphragm arrangement which allows better control of the

post-reflected shock conditions compared to single diaphragm arrangement. The driven section of the shock tube can be pumped down to very low pressures using turbo-pumping to achieve high-purity conditions. A molar ratio of 3.76:1 of $\text{N}_2:\text{O}_2$ was used to prepare TPRF/air mixtures in a magnetically-stirred mixing tank. In the current experiments, the driven section of the shock tube and the mixing tank were heated to 75 °C. The uniformity of the driven section temperature was ensured using various independent temperature controllers. Incident shock speed was measured by six equispaced pressure sensors placed axially along the last 3.7 m from the driven section end-wall. Thermodynamic conditions behind the reflected shock were calculated using standard shock jump relations; estimated uncertainties in pressure and temperature were less than 1%. Ignition delay times were determined using side-wall pressure (1 cm from end-wall) and OH^* chemiluminescence measurements through the side-wall and end-wall ports (see Figure 1). The estimated uncertainty in the shock tube ignition delay measurements is $\pm 20\%$. A gradual pressure rise, dp/dt , of about 2 – 3 %/ ms was observed behind the reflected shock waves. To take this into account, a 3%/ms dp_5/dt was imposed on the constant volume reactor simulations [36]; henceforth referred as ‘shock tube simulations’.

An RCM compresses a fixed mass of premixed fuel/oxidizer/diluent mixture to elevated temperatures and pressures, thereby simulating the compression stroke of an engine cycle. The RCM at NUIG (National University of Ireland, Galway) is different from most other RCMs in that it has a twin-opposed piston configuration, resulting in a relatively fast compression time of about 16 ms. Creviced piston heads were used to increase the post compression temperature homogeneity by suppressing the roll-up vortex in the combustion chamber [37]. The desired conditions at the end of compression can be achieved by varying the compression ratio, the initial pressure (p_0), the initial temperature (T_0) and the diluent gas compositions. The compressed gas temperature, T_c , was calculated using the adiabatic core hypothesis [38]:

$$\int_{T_0}^{T_c} \frac{\gamma}{\gamma - 1} \frac{dT}{T} = \ln \left[\frac{p_c}{p_0} \right]$$

where p_c refers to the measured pressure at the end of compression and γ is the ratio of specific heats. Dynamic pressure profiles (see Figure 1) were measured using a piezoelectric pressure transducer (Kistler 603B). Estimated uncertainty in the calculated end of compression temperature, T_c , is ± 5 K. The ignition delay time (τ) is defined as the time difference between

the end of compression and the point of rapid pressure rise due to ignition. The end of compression is identified by the maximum of the pressure profile prior to the ignition event. The local maximum of the derivative of the pressure with respect to time after the end of compression is defined as the point of ignition. The heat loss in the RCM experiments is accounted for in the simulations (henceforth referred as ‘RCM simulations’) by using volume profiles calculated from pressure traces obtained in non-reactive experiments [38]. All non-reactive volume profiles are included in the Supplementary Material. The estimated uncertainty in RCM ignition delay measurements is $\pm 15\%$.

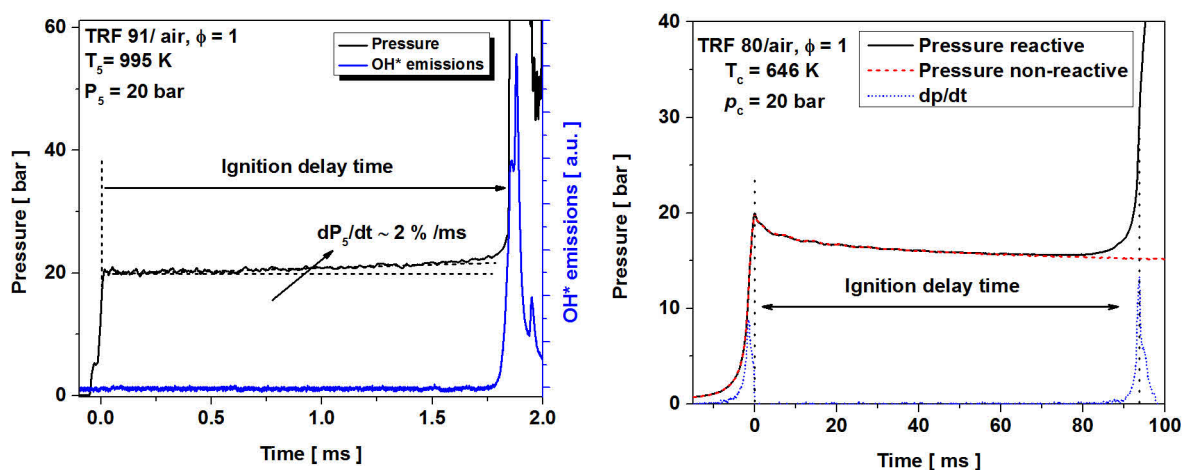


Figure 1: Representative shock tube (left panel) pressure and OH* emission, and RCM (right panel) pressure traces during ignition delay experiments.

3. Results and Discussion

Ignition delay times of TPRF mixtures measured in the HPST and RCM are reported in this section. These data cover a wide range of temperatures (650 – 1250 K), pressures (10, 20 and 40 bar) and equivalence ratios ($\phi = 0.5$ and 1.0). Experiments at 10 bar were only conducted in the RCM as the ignition delay times at low pressures are too long for the shock tube. Throughout this section, the scatter symbols represent the measured data (solid symbols: shock tube data, open symbols: RCM data) and the lines represent the model simulations (solid lines: shock tube simulations, dashed lines: RCM simulations). The gasoline surrogate mechanism developed by Mehl et al. [39] (henceforth referred as ‘LLNL mech’) is used throughout this

manuscript to simulate and interpret the measured data. All the ignition delay data are tabulated in Supplementary Material.

3.1. Effect of Pressure

The effect of pressure (10, 20 and 40 bar) on the ignition delay times of TPRF 70, 80, 91 and 97.5 mixtures is shown in Figure 2 (a) – (d) for the stoichiometric ($\phi = 1$) mixtures, and in Figure 3 (a) – (d) for the fuel-lean ($\phi = 0.5$) cases. The figures show, as expected, that the fuel reactivity increases with increasing pressure at both equivalence ratios. The data show Arrhenius behavior at high ($T > 900$ K) and low ($T < 725$ K) temperatures, and exhibit varying degrees of negative temperature coefficient (NTC) behavior in a temperature range of around 750 – 850 K. The NTC behavior is particularly pronounced at low pressures (10 bar) and for low octane number (and low sensitivity) mixtures (TPRF 70 and 80). The TPRF 97.5 mixture, Figure 2 (d) and Figure 3 (d), showed only marginal NTC behavior. This is due to the high concentration of toluene in the TPRF 97.5 mixture ($\sim 70\%$ vol. toluene, see Table 1), with the low reactivity of toluene suppressing the NTC behavior at all pressures.

The shock tube simulations (solid lines) are in good agreement, both qualitatively and quantitatively, with the HPST data (solid symbols) for the wide range of varying octane number TPRF fuels, Figure 2 and Figure 3 (a) – (d), and adequately capture the pressure dependence of the HPST data. An exception to this trend is the over-prediction of the TPRF 97.5 mixture at $\phi = 1$, Figure 2 (d). This is likely due to the very high content of toluene in this particular mixture and points towards the high-temperature toluene reactivity being too slow in the current model.

The RCM simulations (dashed lines) over-predict the experimental RCM data (open symbols) at low temperatures, particularly for high pressure (20 and 40 bar) and high octane fuels. This over-prediction can be seen clearly for the stoichiometric TPRF 91 and 97.5 mixtures, Figure 2 and Figure 3 (c), (d). For instance, at 700 K, $p = 40$ bar and $\phi = 1$, the mechanism over-predicts RCM ignition delay times of the TPRF 91 and 97.5 mixtures by a factor of 2 and 3, respectively. The observed disagreement may be due to a few things. The mechanism for one or more of the surrogate components (e.g. toluene) may not be appropriately valid across the temperature range. Pressure dependence is certainly included in the model, particularly by the reactions $\dot{\text{H}} + \text{O}_2 (+\text{M}) = \text{H}\dot{\text{O}}_2 (+\text{M})$ and $\text{H}_2\text{O}_2 (+\text{M}) = \dot{\text{O}}\text{H} + \dot{\text{O}}\text{H} (+\text{M})$. However, some pressure dependence may arise due to the $\text{R} + \text{O}_2 \rightleftharpoons \text{RO}_2$ and $\text{QOOH} + \text{O}_2 \rightleftharpoons \dot{\text{O}}_2\text{QOOH}$ equilibria. Given

that the chemistry for hydrogen and syngas has been validated previously, the equilibria for $R + O_2 \rightleftharpoons RO_2$ and $QOOH + O_2 \rightleftharpoons \dot{O}_2QOOH$ need to be further refined.

At 10 bar, we observe opposite trend where the RCM simulations under-predict the ignition delay times in the NTC region and at lower temperatures. In general, the model predictions appear reasonable and perhaps require only minor adjustments at low temperatures for high toluene concentration TPRF fuels at stoichiometric and/or fuel-rich conditions (i.e. at high fuel concentrations). These adjustments may require separate optimization of the toluene sub-mechanism for an improved prediction of the TPRF blends. Toluene sub-chemistry is being separately updated by the NUIG group currently.

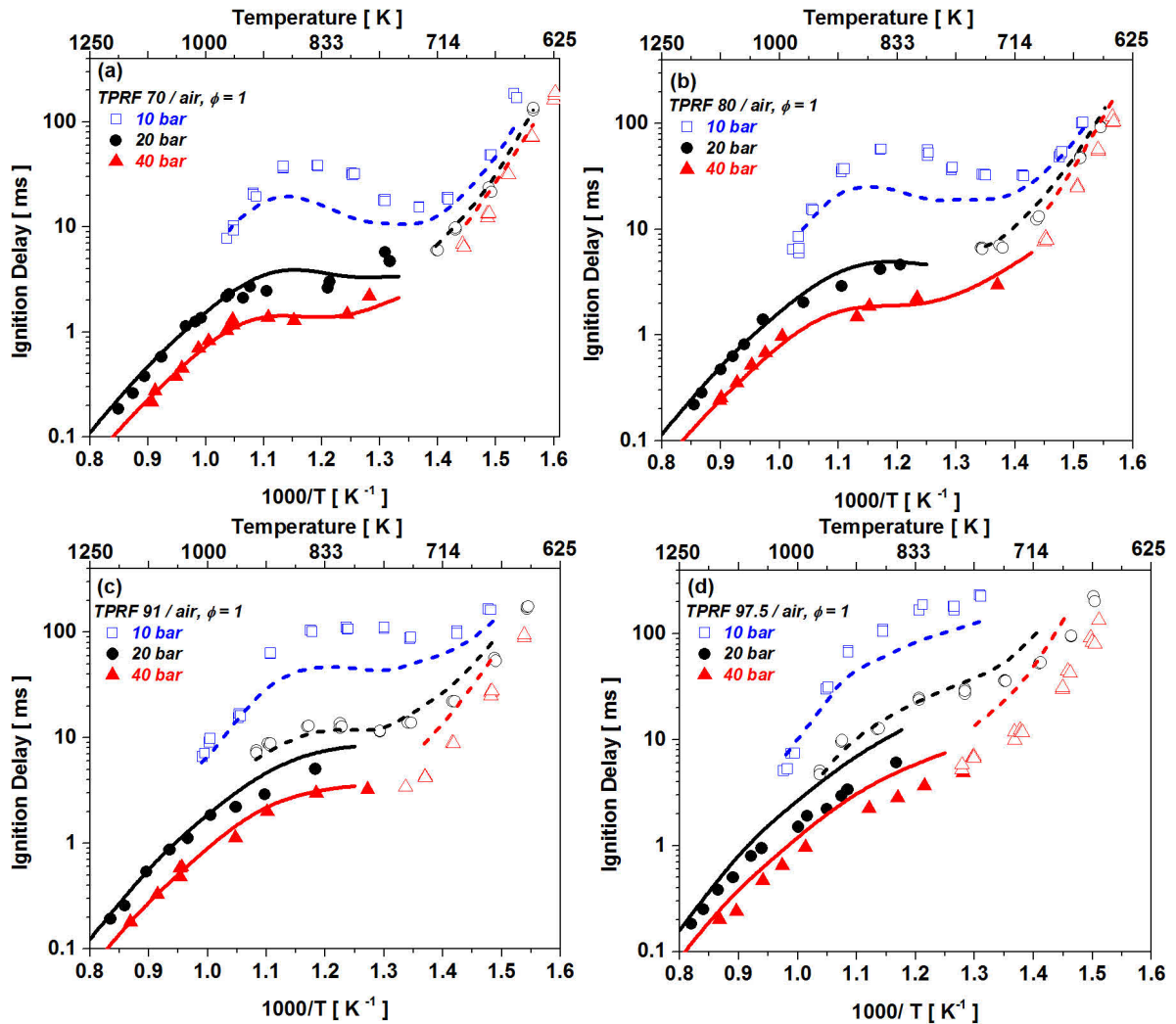


Figure 2: Effect of pressure (10, 20, 40 bar), at $\phi = 1$, on the ignition delay times of (a) TPRF 70, (b) TPRF 80, (c) TPRF 91, (d) TPRF 97.5. Scatter: solid symbols – HPST data, open symbols –

RCM data. Lines: solid lines – shock tube simulations, dashed lines – RCM simulations. LLNL mech [39] is used for simulations.

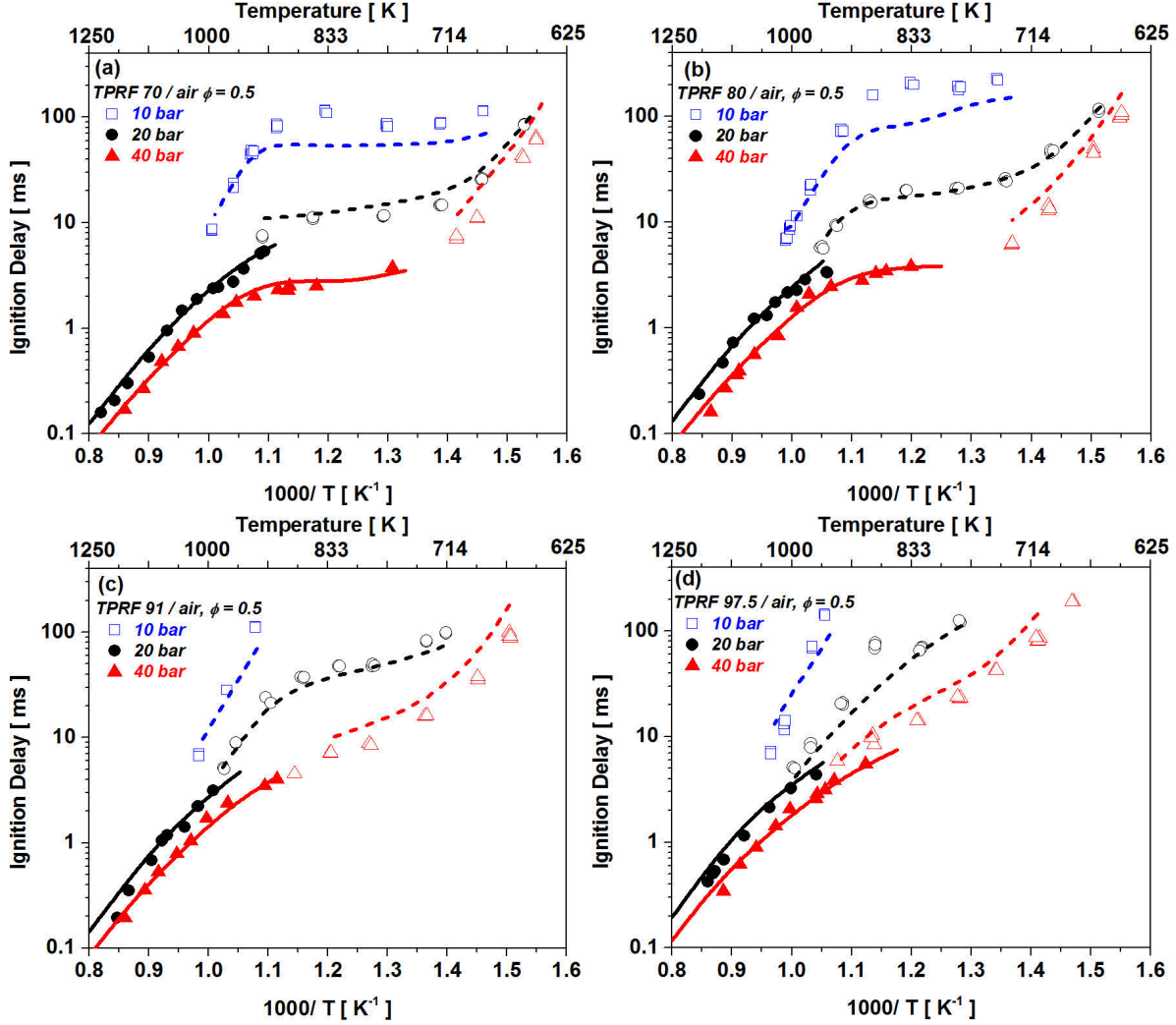


Figure 3: Effect of pressure (10, 20, 40 bar), at $\phi = 0.5$, on the ignition delay times of (a) TPRF 70, (b) TPRF 80, (c) TPRF 91, (d) TPRF 97.5. Scatter: solid symbols – HPST data, open symbols – RCM data. Lines: solid lines – shock tube simulations, dashed lines – RCM simulations. LLNL mech [39] is used for simulations.

Although general agreement between the ignition data from the HPST (KAUST) and RCM (NUIG) is good (Figure 2 and Figure 3), some discrepancies between the two facilities were observed. These are evident at 20 bar in the temperature range of 850 – 1000 K, particularly for the TPRF 91 and 97.5 mixtures at $\phi = 1$, Figure 2 (c), (d), where there is approximately a factor of two difference between the HPST and RCM ignition delay times, with the HPST data being

faster. The authors of this study internally debated various causes and remedies of these discrepancies. For example, careful cross experimentation and validations were performed at the KAUST RCM and the NUIG shock tube (see Supplementary Material Fig. S1). These cross validation experiments revealed similar discrepancies. It is important to note here that this is not the first time such discrepancies are observed between shock tube and RCM data. Recently, Sarathy et al. [41] found similar discrepancies between the shock tubes (Rensselaer Polytechnic Institute, KAUST) and RCM (University of Connecticut) ignition delay times of FACE (Fuels for Advanced Combustion Engines) gasoline F and G at 20 bar and 800 – 1000 K. It can be hypothesized that the homogeneous core model used to simulate RCM data is not fully valid under such conditions; sample RCM pressure profiles are provided in the Supplementary Material (Figs. S3-S14). On the other hand, the relatively long ignition delay shock tube data could potentially be affected by localized flame initiation and propagation [42] resulting in shortened ignition delay times (see Supplementary Material Fig. S2). The discrepancies between shock tube and RCM data under specific conditions are being investigated in a larger collaborative framework and is beyond the scope of this work. Nonetheless, it is important to highlight systematic differences seen between commonly used fundamental experimental devices.

3.2. Effect of Equivalence Ratio

The effect of equivalence ratio ($\phi = 0.5$ and 1.0) on the ignition delay times of TPRF 70, 80, 91 and 97.5 mixtures is shown in Figure 4 – Figure 6 at 10, 20 and 40 bar, respectively. The figures show that, in general, the ignition delay times decrease with increasing equivalence ratio at all pressures and temperatures, i.e., fuel-lean mixtures are slower to ignite compared to stoichiometric ones. At higher temperatures ($T > 1000$ K), the HPST ignition delay data and the simulations show relatively weak dependence on equivalence ratio, with the stoichiometric mixtures being only marginally more reactive compared to the fuel-lean ones at all three pressures. Moreover, this high-temperature equivalence ratio dependence is more pronounced for the high-toluene blend TPRF 97.5 at 40 bar, Figure 6 (d). Similarly, the low-temperature ($T < 725$ K) RCM ignition delay data and simulations show a weak dependence on equivalence ratio, and again the TPRF 97.5 mixture shows the largest variation with equivalence ratio at low temperatures. The dependence on equivalence ratio is most pronounced in the NTC region.

Moreover, in this region, the ϕ -dependence correlates well with the inherent NTC nature of the fuel, i.e., TPRF 70 and 80, Figure 4 – Figure 6 (a), (b), have the most paraffinic content and, therefore, exhibit the largest dependence on equivalence ratio compared to the TPRF 97.5 mixtures, Figure 4 – Figure 6 (d), which have the highest concentrations of toluene and so exhibit the least NTC behavior and the least dependence on equivalence ratio in the NTC region.

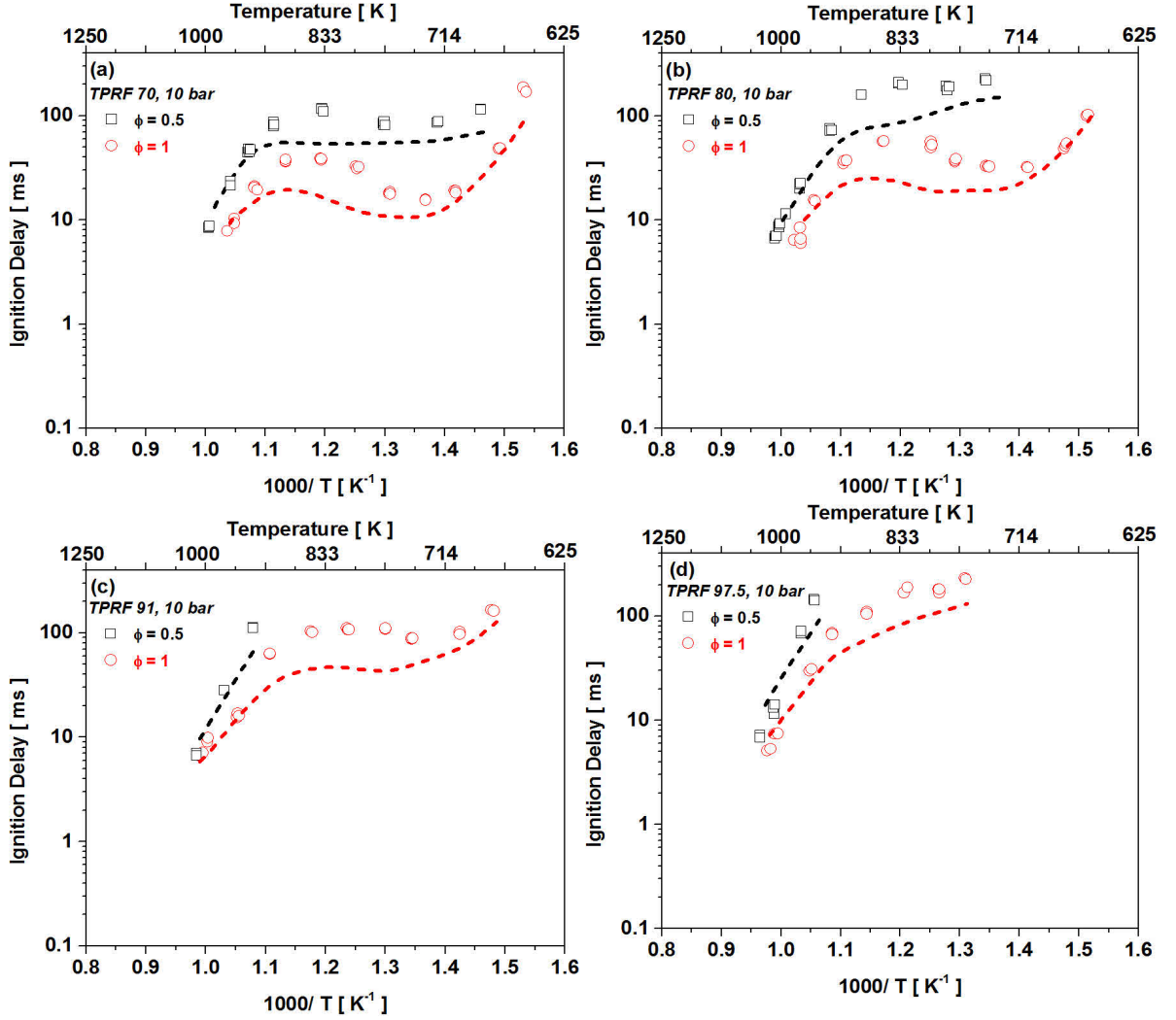


Figure 4: Effect of equivalence ratio ($\phi = 0.5$ and 1.0), at 10 bar, on the ignition delay times of (a) TPRF 70, (b) TPRF 80, (c) TPRF 91, (d) TPRF 97.5. Scatter: open symbols – RCM data. Lines: dashed lines – RCM simulations. LLNL mech [39] is used for simulations. Ignition delay times were not measured in the shock tube for 10 bar.

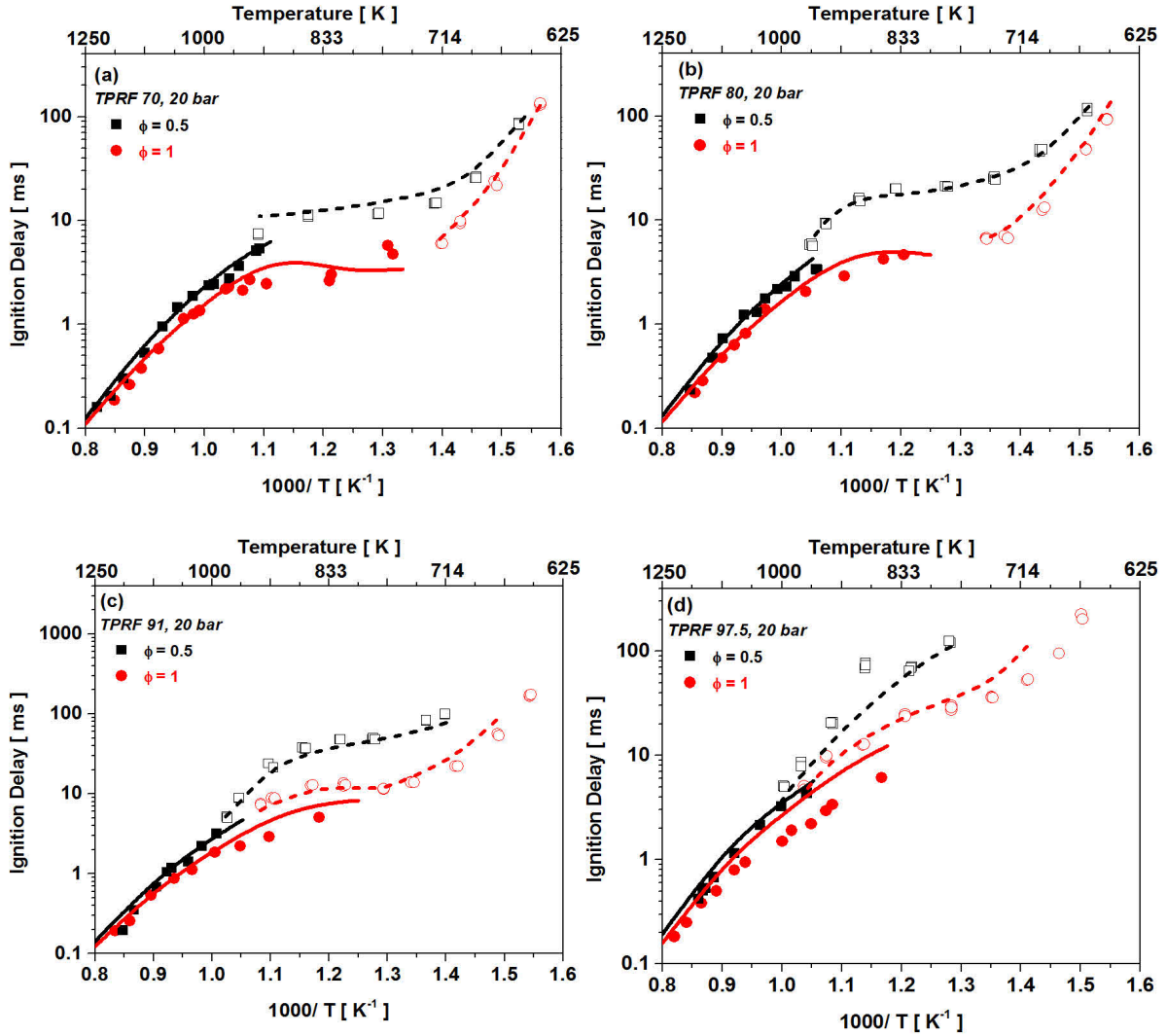


Figure 5: Effect of equivalence ratio ($\phi = 0.5$ and 1.0), at 20 bar, on the ignition delay times of (a) TPRF 70, (b) TPRF 80, (c) TPRF 91, (d) TPRF 97.5. Scatter: solid symbols – HPST data, open symbols – RCM data. Lines: solid lines – shock tube simulations, dashed lines – RCM simulations. LLNL mech [39] is used for simulations.

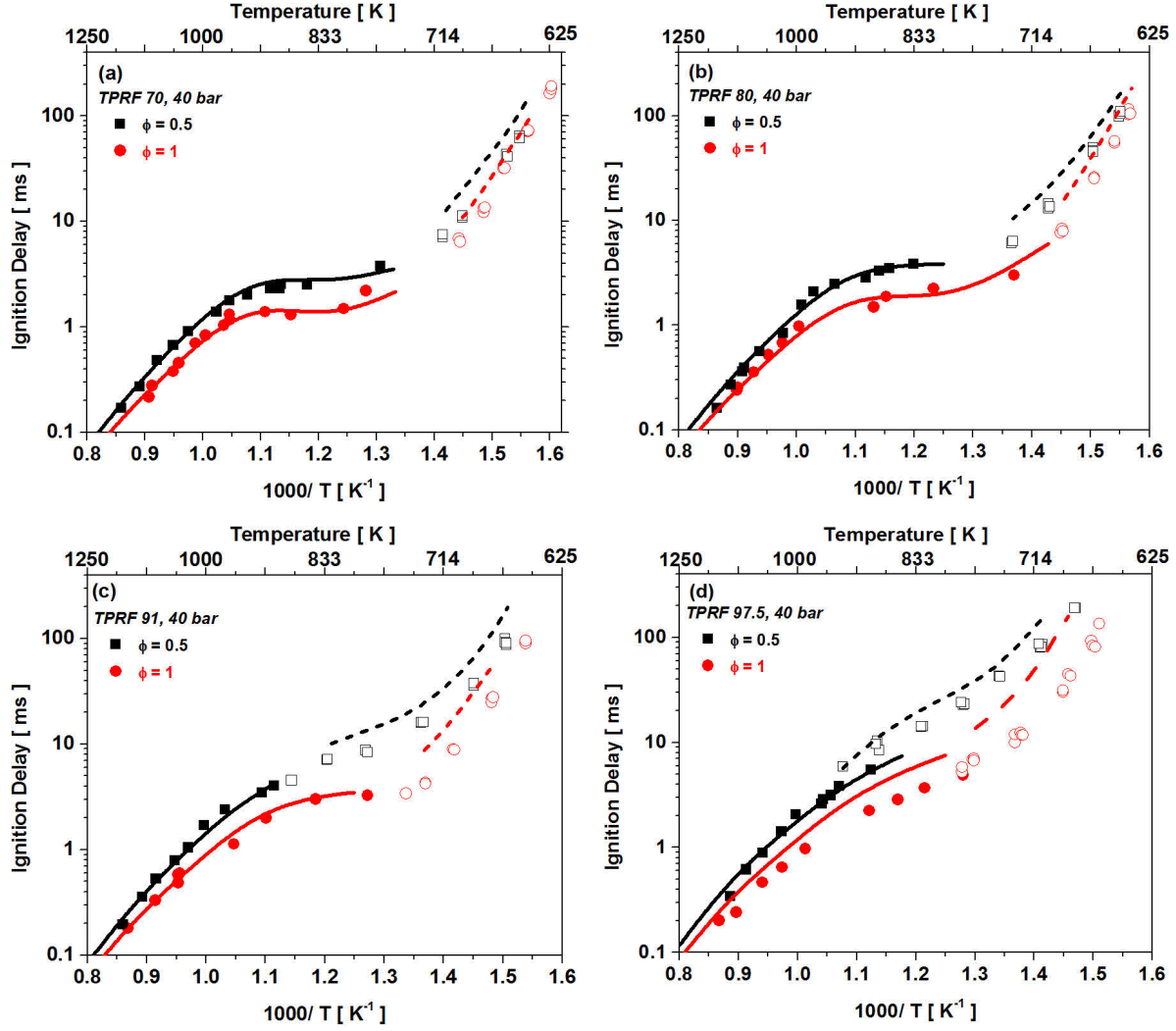


Figure 6: Effect of equivalence ratio ($\phi = 0.5$ and 1.0), at 40 bar, on the ignition delay times of (a) TPRF 70, (b) TPRF 80, (c) TPRF 91, (d) TPRF 97.5. Scatter: solid symbols – HPST data, open symbols – RCM data. Lines: solid lines – shock tube simulations, dashed lines – RCM simulations. LLNL mech [39] is used for simulations.

3.3. Effect of Octane Number

The effect of octane number on ignition delay times of TPRF 70, 80, 91 and 97.5 mixtures is shown in Figure 7 (for $\phi = 1$) and Figure 8 (for $\phi = 0.5$). The figures show that at high temperatures ($T > 1000$ K), the measured and simulated ignition delay times of all of the fuels show very similar ignition delay times. At very low temperatures ($T < 700$ K), the measured and simulated ignition delay times show a weak dependence on the research octane number (RON)

of the fuel. At low temperatures, this octane dependence is more pronounced for the higher RON fuels i.e., there is on average a factor of 2 – 3 difference between the ignition delay times of TPRF 97.5 (RON 97.5) and TPRF 91 (RON 91) mixtures. This difference diminishes as we move to lower RON fuels, as can be seen by the negligible reactivity differences between TPRF 80 (RON 80) and TPRF 70 (RON 70). Another way to consider this reactivity difference at low temperatures is by looking at the sensitivity of these fuels. The sensitivity of the studied fuels decreases from TPRF 97.5 ($S = 10.9$) to TPRF 70 ($S = 4$). This indicates that large reactivity differences at low temperatures for TPRF 97.5 and TPRF 91 mixtures compared to TPRF 80 and TPRF 70 mixtures are primarily driven by the non-paraffinic content (toluene) present in these fuels. Therefore, it can be argued that, at low temperatures, the octane dependence of TPRFs will only be significant for high sensitivity TPRF fuels, i.e., fuels composed of a large non-paraffinic content.

The largest effect of octane number on the reactivity (ignition delay times) is observed in the NTC region (near 750 – 850 K). It can be seen clearly in Figure 7 (for $\phi = 1$) and Figure 8 (for $\phi = 0.5$) that the ignition delay times correlate very well with the octane number of these fuels, i.e., the fuel with the highest octane number (RON) has the longest ignition delay times and the reactivity increases (ignition delay time decreases) with a decrease in octane number (RON). Mehl et al. [43, 44] have shown that ignition delay times in the NTC region (at 825 K and 25 atm) correlate well with the RON of fuels. Sarathy et al. [45] and Badra et al. [46] also formulated methodologies to correlate NTC region ignition delay times to RON and MON. The results from the current study also confirm that correlations between octane ratings (RON, MON, S) and ignition delay times for TPRF surrogates can be best formulated in the NTC region.

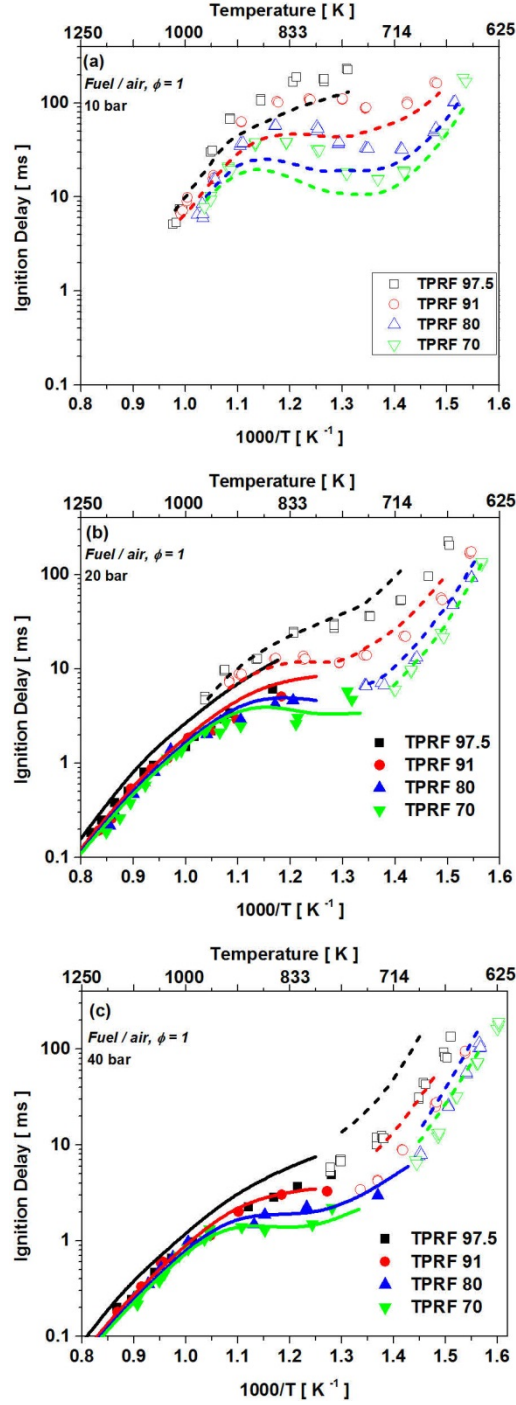


Figure 7: Effect of RON (97.5, 91, 80, 70), at $\phi = 1$, on the ignition delay times of TPRF 97.5 (■), TPRF 91 (●), TPRF 80 (▲), TPRF 70 (▼) at (a) 10 bar, (b) 20 bar and (c) 40 bar. Scatter: solid symbols – HPST data, open symbols – RCM data. Lines: solid lines – shock tube simulations, dashed lines – RCM simulations. LLNL mech [39] is used for simulations.

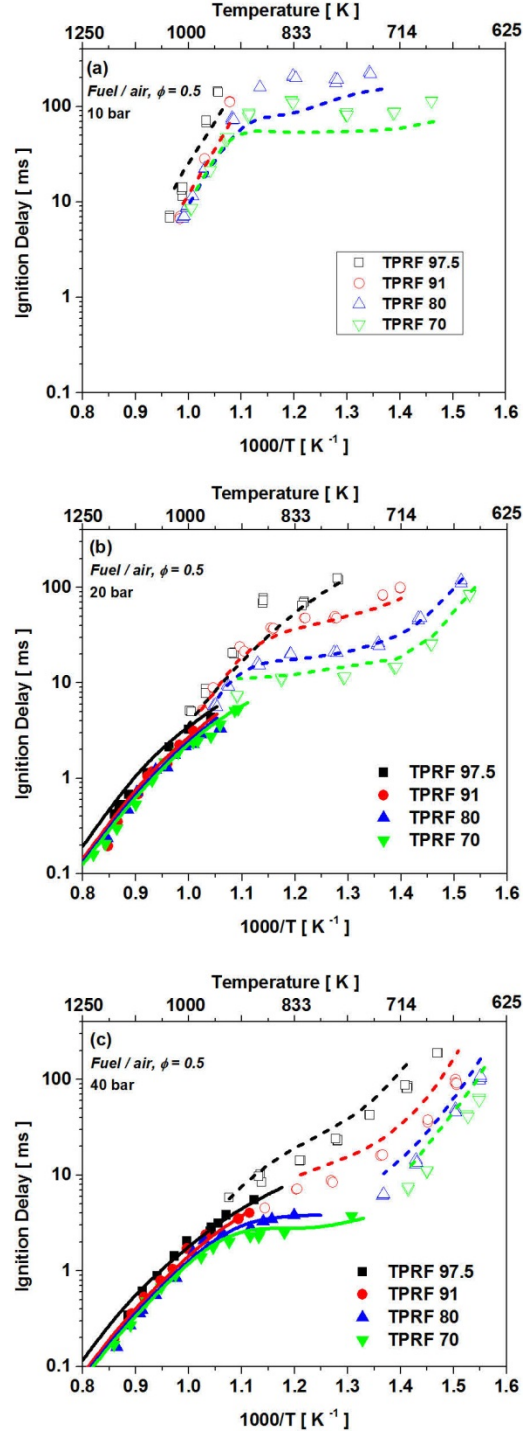


Figure 8: Effect of RON (97.5, 91, 80, 70), at $\phi = 0.5$, on the ignition delay times of TPRF 97.5 (■), TPRF 91 (●), TPRF 80 (▲), TPRF 70 (▼) at (a) 10 bar, (b) 20 bar and (c) 40 bar. Scatter: solid symbols – HPST data, open symbols – RCM data. Lines: solid lines – shock tube simulations, dashed lines – RCM simulations. LLNL mech [39] is used for simulations.

4. Chemical Kinetic Analyses

In the previous section (Section 3.3), several observations were made about the dependence of ignition delay times of the TPRFs on the octane number of the fuel. Firstly, at high temperatures, very little effect of octane number on the ignition delay times was observed. Furthermore, at low temperatures, a weak octane number dependence was observed, and this dependence was pronounced for high-RON and high-sensitivity fuels (TPRF 97.5, TPRF 91) compared to low-RON and low-sensitivity fuels (TPRF 80, TPRF 70). Finally, a strong dependence of octane number on the ignition delay times was observed in the NTC region. We will now explain these trends using chemical kinetic analyses.

At high temperatures ($T > 1000$ K), ignition is primarily controlled by the thermal chain branching of H_2O_2 to produce two $\dot{\text{O}}\text{H}$ radicals via the reaction $\text{H}_2\text{O}_2 (+\text{M}) \leftrightarrow \dot{\text{O}}\text{H} + \dot{\text{O}}\text{H} (+\text{M})$, which is favored more or less equally for various fuels studied here. This results in very similar ignition delay times at high temperatures and hence an almost indistinguishable dependence of ignition delay times on octane number at high temperatures.

At low temperatures ($T < 700$ K), degenerate chain branching to produce $\dot{\text{O}}\text{H}$ radicals primarily controls the ignition of typical paraffinic fuels [47]. A rate of production (ROP) analyses based on $\dot{\text{O}}\text{H}$ radicals are utilized here (Figure 9) to highlight key similarities and differences between the various fuels studied here. There is significant temperature rise associated with ignition (first and second stage). Therefore, to assess the effects of kinetics on the ignition process, any kinetic analysis should be performed at times adequately before the ignition associated temperature rise. In this work the ROP analyses are performed at times corresponding to 2/3 of exponential OH radicals buildup which also roughly corresponds to 2/3 of ignition delay time, and hence have negligible effects temperature rise associated with ignition (first and second stage). This definition is in line with the guidelines provided by Merchant et al. [48]. It can be seen that H-abstraction from the fuel (*n*-heptane/iso-octane/toluene) is responsible for $\dot{\text{O}}\text{H}$ radical consumption (negative ROP) for all cases. However, these consumption channels are widely different as we go from high-RON, high-sensitivity fuels (TPRF 97.5, TPRF 91) to low-RON, low-sensitivity fuels (TPRF 70, TPRF 80). Figure 9 (c) and (d) show that H-abstraction by $\dot{\text{O}}\text{H}$ radicals from toluene to produce benzyl radical is the most important $\dot{\text{O}}\text{H}$ radical consumption channel for TPRF 97.5 and TPRF 91 mixtures; however, H-abstraction from secondary sites on *n*-heptane to produce *n*-heptyl radicals are the most important $\dot{\text{O}}\text{H}$

consumption pathways for the TPRF 80 and 70 mixtures (Figure 9 (a) and (b)). The subsequent pathways for these radicals (abstraction products) control the low-temperature ignition process. The benzyl radicals formed by H-atom abstraction are stabilized [23] at low temperatures rendering toluene or high toluene-containing fuels (like TPRF 97.5 mixtures in this case) relatively un-reactive at lower temperatures. The subsequent ignition of high toluene concentration fuels, even at low temperatures, is controlled by H_2O_2 decomposition due to the temperature increase associated with the exothermicity of the oxidation of toluene to benzyl radical (and subsequently benzylaldehyde) and water [23]. On the other hand, the highly reactive *n*-heptyl radicals formed by H-abstraction by $\dot{\text{O}}\text{H}$ radicals in the TPRF 80 and 70 mixtures follow the expected low-temperature degenerate chain branching pathways [47] to produce $\dot{\text{O}}\text{H}$ radicals (positive ROP). The *n*-heptyl radicals react with molecular oxygen to form alkylperoxy radicals, which then undergo a series of isomerization and oxygen addition reactions to form ketohydroperoxides (KHPs) and $\dot{\text{O}}\text{H}$ radicals. The decomposition of KHPs produces additional $\dot{\text{O}}\text{H}$ radicals, resulting in an exponential growth of $\dot{\text{O}}\text{H}$ radicals and ignition. It can be concluded from the ROP analyses that *n*-heptane primarily controls $\dot{\text{O}}\text{H}$ consumption for TPRFs with low sensitivity / low RON (TPRFs 70 and 80) and, therefore, relatively weak octane dependence is seen at low temperatures for these low sensitivity TPRFs. On the other hand, significant octane dependence observed for the high sensitivity / high RON TPRFs may be attributed to the toluene kinetics.

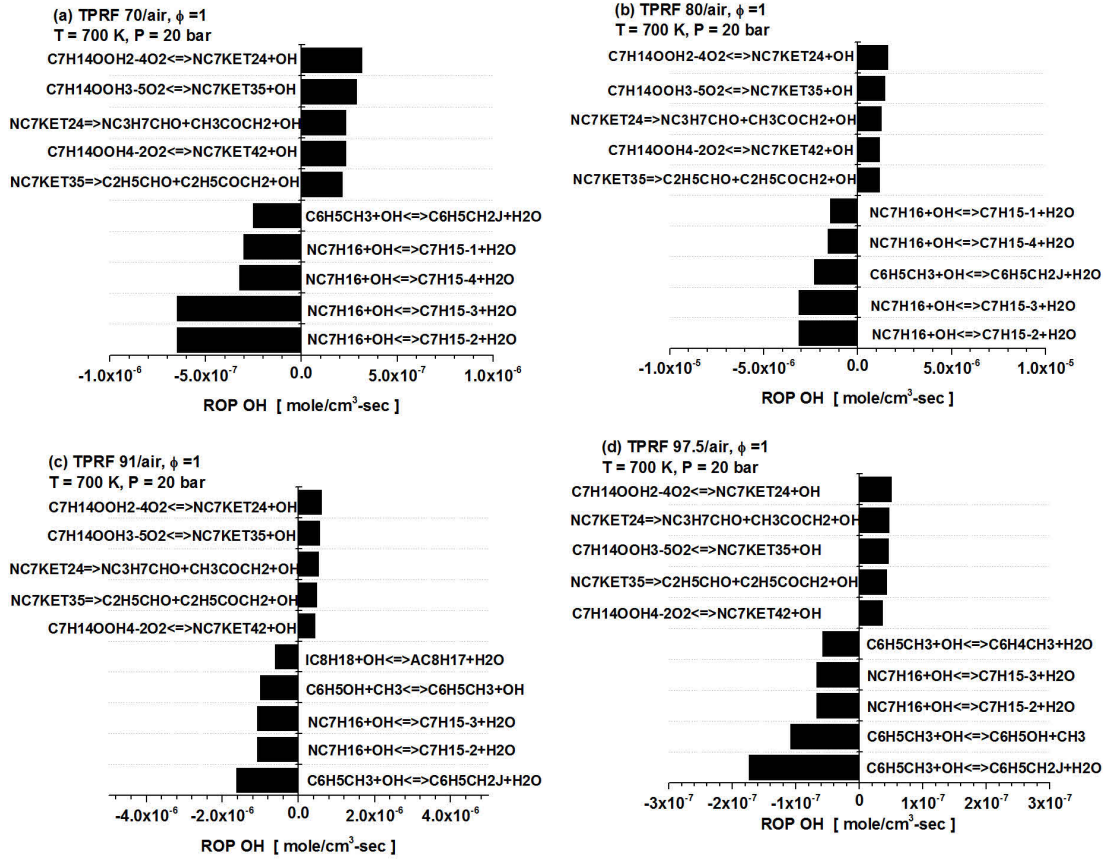


Figure 9: ROP analyses of $\dot{O}H$ radical at $T = 700 \text{ K}$, $p = 20 \text{ bar}$, $\phi = 1$; (a) TPRF 70/air, (b) TPRF 80/air, (c) TPRF 91/air, and (d) TPRF 97.5/air mixtures. LLNL mech [39] is used for ROP analyses. The ROP analyses are conducted at a time corresponding to two-thirds of the exponential growth of $\dot{O}H$ radical concentration

At intermediate temperatures (750 – 850 K), $\dot{H}O_2$ radicals are primarily produced through ($\dot{R}O_2 \leftrightarrow \text{alkene} + \dot{H}O_2$) or ($R + O_2 \leftrightarrow \text{alkene} + \dot{H}O_2$) concerted elimination mechanisms [47]. Production of $\dot{H}O_2$ radicals, through either mechanism, renders the system unreactive and is the main cause of the NTC behavior. Once formed, $\dot{H}O_2$ radicals are mainly converted to H_2O_2 ($RH + \dot{H}O_2 \leftrightarrow R + H_2O_2$), and, therefore, the eventual chain branching of H_2O_2 to produce two $\dot{O}H$ radicals controls ignition in the NTC region. Figure 10 shows the $\dot{H}O_2$ ROP analyses for various TPRF fuels examined in this study. It can be seen that $\dot{H}O_2$ radical production (positive ROP) is favored much more for the TPRF 70 mixture compared to the other mixtures, and as such it correlates well with the RON and sensitivity of the TPRF fuels (smaller the RON and sensitivity, larger the $\dot{H}O_2$ radical production). This is why both experimental data and simulations in the

previous section showed enhanced NTC behavior for TPRF 70 mixtures compared to the other ternary blends. It can also be seen in Figure 10 that the production of $\dot{\text{H}}\text{O}_2$ radicals is much lower for TPRF 97.5 mixture compared to other fuels, and this is the primary reason for the near negligible NTC behavior for TPRF 97.5. Moreover, the figure also shows that the consumption of $\dot{\text{H}}\text{O}_2$ radicals (negative ROP) to produce H_2O_2 and its further decomposition to two $\dot{\text{O}}\text{H}$ radicals (not shown here) are much more favored for TPRF 70 mixtures compared to others. This is the primary reason for the increased reactivity (shorter ignition delay times) of TPRF 70 mixtures compared to other fuels in the NTC region.

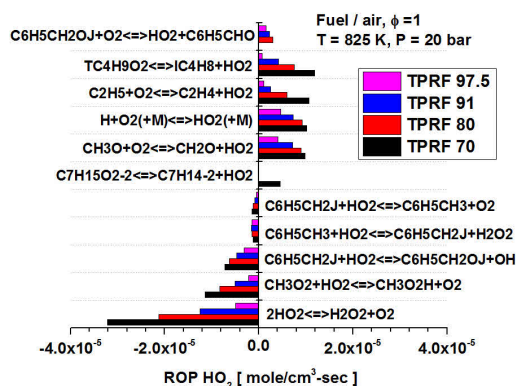


Figure 10: ROP analysis of $\dot{\text{H}}\text{O}_2$ radical at $T = 825 \text{ K}$, $p = 20 \text{ bar}$, $\phi = 1$ for TPRF 97.5/air (magenta bars), TPRF 91/air (blue bars), TPRF 80/air (red bars), and TPRF 70/air (black bars) mixtures. LLNL mech [39] is used for ROP analysis. The ROP analyses are conducted at the time corresponding to two-thirds of the exponential growth of $\dot{\text{H}}\text{O}_2$ radical concentration

5. Conclusions

Ignition delay times of a wider range of toluene/iso-octane/n-heptane mixtures (TPRFs) have been measured in this study. The LLNL mech [39] was used to simulate and interpret these data. It is shown that the mechanism predictions are in good agreement with the shock tube data but improvements are necessary to better simulate the low-temperature RCM data. Refinements in the mechanism are particularly required to simulate the high toluene content fuels. It is shown that the TPRF fuels show a negligible octane dependence at high temperatures, a weak octane dependence at low temperatures and a strong octane dependence in the NTC region. At low temperatures, the octane dependence is more pronounced for the high-RON, high-sensitivity fuels and is attributed to the non-paraffinic (toluene) content. In the NTC region, the fuels with low RON and low sensitivity produce larger concentrations of $\dot{\text{H}}\text{O}_2$ and H_2O_2 , and hence show

the most prominent NTC behavior and ignition advancement compared to the high-RON, high-sensitivity fuels. These comprehensive ignition delay time measurements provide highly valuable benchmark datasets for further development and validation of gasoline surrogate mechanisms.

Acknowledgements

Research reported in this paper was funded by Saudi Aramco under the FUELCOM program and by King Abdullah University of Science and Technology (KAUST).

References

- [1] W.J. Pitz, N.P. Cernansky, F.L. Dryer, F. Egolfopoulos, J. Farrell, D. Friend, H. Pitsch, SAE 2007-01-0175.
- [2] T. Wallington, E. Kaiser, J. Farrell, Automotive fuels and internal combustion engines: a chemical perspective, *Chem. Soci. Rev.*, 35 (2006) 335-347.
- [3] M. Christensen, B. Johansson, P. Einewall, SAE 972874., (1997).
- [4] K. Epping, S. Aceves, R. Bechtold, J.E. Dec, SAE 2002-01-1923.
- [5] R.H. Stanglmaier, C.E. Roberts, SAE 1999-01-3682.
- [6] T. Aoyama, Y. Hattori, J.i. Mizuta, Y. Sato, SAE 960081., (1996).
- [7] M. Jia, M. Xie, A chemical kinetics model of iso-octane oxidation for HCCI engines, *Fuel*, 85 (2006) 2593-2604.
- [8] J. Badra, A. Elwardany, J. Sim, Y. Viollet, H. Im, J. Chang, Effects of In-Cylinder Mixing on Low Octane Gasoline Compression Ignition Combustion, in, SAE Technical Paper, 2016.
- [9] S. Dooley, S.H. Won, M. Chaos, J. Heyne, Y. Ju, F.L. Dryer, K. Kumar, C.-J. Sung, H. Wang, M.A. Oehlschlaeger, A jet fuel surrogate formulated by real fuel properties, *Combust. Flame*, 157 (2010) 2333-2339.
- [10] A. Ahmed, G. Goteng, V.S. Shankar, K. Al-Qurashi, W.L. Roberts, S.M. Sarathy, A computational methodology for formulating gasoline surrogate fuels with accurate physical and chemical kinetic properties, *Fuel*, 143 (2015) 290-300.
- [11] C.J. Mueller, W.J. Cannella, T.J. Bruno, B. Bunting, H.D. Dettman, J.A. Franz, M.L. Huber, M. Natarajan, W.J. Pitz, M.A. Ratcliff, Methodology for formulating diesel surrogate fuels with accurate compositional, ignition-quality, and volatility characteristics, *Energy Fuels*, 26 (2012) 3284-3303.
- [12] D. Kim, J. Martz, A. Violi, A surrogate for emulating the physical and chemical properties of conventional jet fuel, *Combust. Flame*, 161 (2014) 1489-1498.
- [13] G. Kalghatgi, H. Babiker, J. Badra, A Simple Method to Predict Knock Using Toluene, N-Heptane and Iso-Octane Blends (TPRF) as Gasoline Surrogates, *SAE Int. Journ. Engines*, 8 (2015) 505-519.
- [14] G. Kalghatgi, R. Head, J. Chang, Y. Viollet, H. Babiker, A. Amer, An alternative method based on toluene/n-heptane surrogate fuels for rating the anti-knock quality of practical gasolines, *SAE Int. Journ. Fuels Lubricants*, 7 (2014) 663-672.

- [15] H. Ciezki, G. Adomeit, Shock-tube investigation of self-ignition of n-heptane-air mixtures under engine relevant conditions, *Combust. Flame*, 93 (1993) 421-433.
- [16] K. Fieweger, R. Blumenthal, G. Adomeit, Self-ignition of SI engine model fuels: A shock tube investigation at high pressure, *Combust. Flame*, 109 (1997) 599-619.
- [17] R. Minetti, M. Carlier, M. Ribaucour, E. Therssen, L. Sochet, A rapid compression machine investigation of oxidation and auto-ignition of n-heptane: measurements and modeling, *Combust. Flame*, 102 (1995) 298-309.
- [18] H. Curran, P. Gaffuri, W.J. Pitz, C.K. Westbrook, A comprehensive modeling study of n-heptane oxidation, *Combust. Flame*, 114 (1998) 149-177.
- [19] H.J. Curran, P. Gaffuri, W. Pitz, C. Westbrook, A comprehensive modeling study of iso-octane oxidation, *Combust. Flame*, 129 (2002) 253-280.
- [20] E. Ranzi, P. Gaffuri, T. Faravelli, P. Dagaut, A wide-range modeling study of n-heptane oxidation, *Combust. Flame*, 103 (1995) 91-106.
- [21] E. Ranzi, T. Faravelli, P. Gaffuri, A. Sogaro, A. D'Anna, A. Ciajolo, A wide-range modeling study of iso-octane oxidation, *Combust. Flame*, 108 (1997) 24-42.
- [22] H.J. Curran, W. Pitz, C. Westbrook, G. Callahan, F. Dryer, Oxidation of automotive primary reference fuels at elevated pressures, *Intl. Sympo. Combust.*, 27 (1998) 379-387.
- [23] G. Vanhove, G. Petit, R. Minetti, Experimental study of the kinetic interactions in the low-temperature autoignition of hydrocarbon binary mixtures and a surrogate fuel, *Combust. Flame*, 145 (2006) 521-532.
- [24] C. Callahan, T. Held, F. Dryer, R. Minetti, M. Ribaucour, L. Sochet, T. Faravelli, P. Gaffuri, E. Rani, Experimental data and kinetic modeling of primary reference fuel mixtures, in: *Symposium (International) on Combustion*, Elsevier, 1996, pp. 739-746.
- [25] S. Tanaka, F. Ayala, J.C. Keck, J.B. Heywood, Two-stage ignition in HCCI combustion and HCCI control by fuels and additives, *Combust. Flame*, 132 (2003) 219-239.
- [26] F. Buda, R. Bounaceur, V. Warth, P.-A. Glaude, R. Fournet, F. Battin-Leclerc, Progress toward a unified detailed kinetic model for the autoignition of alkanes from C 4 to C 10 between 600 and 1200 K, *Combust. Flame*, 142 (2005) 170-186.
- [27] L. Cai, H. Pitsch, Optimized chemical mechanism for combustion of gasoline surrogate fuels, *Combust. Flame*, 162 (2015) 1623-1637.
- [28] S.M. Sarathy, G. Kukkadapu, M. Mehl, W. Wang, T. Javed, S. Park, M.A. Oehlschlaeger, A. Farooq, W.J. Pitz, C.-J. Sung, Ignition of alkane-rich FACE gasoline fuels and their surrogate mixtures, *Proci. Combust. Inst.*, 35 (2015) 249-257.
- [29] B. Gauthier, D. Davidson, R. Hanson, Shock tube determination of ignition delay times in full-blend and surrogate fuel mixtures, *Combust. Flame*, 139 (2004) 300-311.
- [30] G. Kukkadapu, K. Kumar, C.-J. Sung, M. Mehl, W.J. Pitz, Experimental and surrogate modeling study of gasoline ignition in a rapid compression machine, *Combust. Flame*, 159 (2012) 3066-3078.
- [31] G. Kukkadapu, K. Kumar, C.-J. Sung, M. Mehl, W.J. Pitz, Autoignition of gasoline and its surrogates in a rapid compression machine, *Proci. Combust. Inst.*, 34 (2013) 345-352.
- [32] G. Kukkadapu, K. Kumar, C.-J. Sung, M. Mehl, W.J. Pitz, Autoignition of gasoline surrogates at low temperature combustion conditions, *Combust. Flame*, 162 (2015) 2272-2285.
- [33] N. Morgan, A. Smallbone, A. Bhawe, M. Kraft, R. Cracknell, G. Kalghatgi, Mapping surrogate gasoline compositions into RON/MON space, *Combust. Flame*, 157 (2010) 1122-1131.
- [34] C. Pera, V. Knop, Methodology to define gasoline surrogates dedicated to auto-ignition in engines, *Fuel*, 96 (2012) 59-69.

- [35] S.M. Burke, U. Burke, R. Mc Donagh, O. Mathieu, I. Osorio, C. Keesee, A. Morones, E.L. Petersen, W. Wang, T.A. DeVerter, An experimental and modeling study of propene oxidation. Part 2: Ignition delay time and flame speed measurements, *Combust. Flame*, 162 (2015) 296-314.
- [36] M. Chaos, F.L. Dryer, Chemical-kinetic modeling of ignition delay: Considerations in interpreting shock tube data, *International Journal of Chemical Kinetics*, 42 (2010) 143-150.
- [37] L. Brett, J. MacNamara, P. Musch, J. Simmie, Simulation of methane autoignition in a rapid compression machine with creviced pistons, *Combust. Flame*, 124 (2001) 326-329.
- [38] G. Mittal, C.-J. SUNG*, A rapid compression machine for chemical kinetics studies at elevated pressures and temperatures, *Combust. Sci. Tech.*, 179 (2007) 497-530.
- [39] M. Mehl, W.J. Pitz, C.K. Westbrook, H.J. Curran, Kinetic modeling of gasoline surrogate components and mixtures under engine conditions, *Proci. Combust. Inst.*, 33 (2011) 193-200.
- [40] Z. Wang, S.M. Sarathy, Third O₂ addition reactions promote the low-temperature auto-ignition of n-alkanes, *Combust. Flame*, (2016).
- [41] S.M. Sarathy, G. Kukkadapu, T. Javed, A. Ahmed, A. Tekawade, M. Mehl, G. Kosiba, S. Park, M.A. Rashidi, W.L. Roberts, M.A. Oehlschlaeger, C.-J. Sung, A. Farooq, *Combust. Flame*, (Submitted November, 2015).
- [42] Y. Uygun, S. Ishihara, H. Olivier, A high pressure ignition delay time study of 2-methylfuran and tetrahydrofuran in shock tubes, *Combust. Flame*, 161 (2014) 2519-2530.
- [43] M. Mehl, T. Faravelli, F. Giavazzi, E. Ranzi, P. Scorletti, A. Tardani, D. Terna, Detailed chemistry promotes understanding of octane numbers and gasoline sensitivity, *Energy Fuels*, 20 (2006) 2391-2398.
- [44] M. Mehl, J.-Y. Chen, W.J. Pitz, S. Sarathy, C.K. Westbrook, An approach for formulating surrogates for gasoline with application toward a reduced surrogate mechanism for CFD engine modeling, *Energy Fuels*, 25 (2011) 5215-5223.
- [45] S.M. Sarathy, T. Javed, F. Karsenty, A. Heufer, W. Wang, S. Park, A. Elwardany, A. Farooq, C.K. Westbrook, W.J. Pitz, A comprehensive combustion chemistry study of 2, 5-dimethylhexane, *Combust. Flame*, 161 (2014) 1444-1459.
- [46] J.A. Badra, N. Bokhumseen, N. Mulla, S.M. Sarathy, A. Farooq, G. Kalghatgi, P. Gaillard, A methodology to relate octane numbers of binary and ternary n-heptane, iso-octane and toluene mixtures with simulated ignition delay times, *Fuel*, 160 (2015) 458-469.
- [47] J. Zádor, C.A. Taatjes, R.X. Fernandes, Kinetics of elementary reactions in low-temperature autoignition chemistry, *Prog. Energy. Combust. Sci.*, 37 (2011) 371-421.
- [48] S.S. Merchant, C.F. Goldsmith, A.G. Vandeputte, M.P. Burke, S.J. Klippenstein, W.H. Green, Understanding low-temperature first-stage ignition delay: Propane, *Combust. Flame*, 162 (2015) 3658-3673.